

**EXCESS HEAT EVOLUTION AND ANALYSIS OF ELEMENTS FOR SOLID STATE ELECTROLYTE IN DEUTERIUM ATMOSPHERE DURING APPLIED ELECTRIC FIELD**

Tadahiko Mizuno, Tadashi Akimoto  
Kazuhisa Azumi, Masatoshi Kitaichi, and  
Kazuya Kurokawa  
Hokkaido Univ., Kitaku, North 13 West 8, Sapporo 060 Japan

Michio Enyo  
Hakodate National College of Technology, Tokuracho 14-1, Hakodate 042 Japan

**ABSTRACT**

A proton conductor, the solid state electrolyte, made from oxide of strontium, cerium, niobium and yttrium can be charged in a hot  $D_2$  gas atmosphere to produce excess heat. Anomalous heat evolution was observed for 12 in 80 cases of the samples charged by alternating current for 5 to 45 Volts at temperatures ranging from 400 to 700°C. Several kinds of alkali metals, Ca, Mg, Bismuth, Lantanides and Aluminum were locally segregated and distributed around the melted and swelled parts of the samples that generated an excess heat.

**INTRODUCTION**

The alleged Cold Fusion reaction still has not been confirmed because of lack of data. It is very important to obtain precision relationships quantitatively between each reaction products that may cause the reaction. We understand that the most desirable parameter to analyze the reaction mechanism is to obtain simultaneously all the quantities such as heat evolution, neutron emission, tritium generation, and so on. However, unfortunately, this is very difficult due to difficulties to reproduce and control the phenomena. Even if it has been possible, usually the amounts of reaction products are very low and sometimes nearly or under the detection limit; it is difficult to calibrate quantitatively. Therefore, it is suitable to analyze the element in the sample before and after the experiment.

**EXPERIMENTAL**

Samples were made from a mixture of metal oxide of Sr, Ce, Y and Nb. The procedures were developed by Iwahara et al. [1-3]. These powdered oxides were first mixed, and then sintered in an electric furnace at 1,400° C in air for 16 hours. The samples were pulverized, and mixed, alcohol was added, and the samples were put in a pressing machine and formed into round plates of 20 mm in diameter and 1 mm thick. These plates were again sintered at 1,300-1,480° C in air for 16 hours. Sample densities ranged from 3.0 to 5.2; the theoretical density for perfectly sintered sample is 5.8. Both sides of the sintered sample were then coated with porous Pt film, by painting a Pt organic compound and deposition in 700° C or coated by Ar sputtered to Pt in vacuum. The resulting Pt film thickness was 0.15-0.3  $\mu\text{m}$ . The film is porous and has a very rough surface; Hydrogen gas easily passes through the film and reaches to ceramic surface.

Experimental arrangement is shown in Fig. 1. The sample was heated to a constant temperature with an electric heater covered with stainless steel. Electric power was supplied from a stabilized power source. The electric fields of constant voltage (Electric power of proton driving: EPD) was supplied from a

function generator via a power amplifier. Pressure was measured by a capacitance manometer with 0.1 Torr accuracy. Temperatures were recorded with  $0.1^\circ\text{C}$  accuracy by three thermocouples that were coated by a thin stainless cover. All parameters, EPD (voltage and electric current), heater power, sample temperature, gas pressure and cylinder wall temperature were recorded through a data logger and computer to floppy diskette. The reaction cell is made by a stainless steel cylinder 40 cm long, 20 cm in diameter, with walls 5 mm thick.

Upper part of the cell is shown in Fig. 2. The sample is held on both sides by 0.3 mm thick Pt plates which are in turn sandwiched between 0.3 mm thick Pt plates. Three thermocouples with thin stainless steel are pressed directly on the upper Pt plate. The Pt plates make electrical and thermal contact with ceramic sample and thermocouples. This part is fixed on place of heater part. Spiral heater wire covered with ceramic insulator is also connected to the bottom part of the sample. EPD power was supplied through copper wires of 1.6 mm in diameter. The sample holder is surrounded by Ni plate reflectors. The holder is fixed with four supports made of 6 mm diameter stainless steel rods that were covered by alumina insulator. Four nuts attached under the support rods pressed Pt plate, alumina spacer and sample to make tight contact with thermocouples. These thermocouples have a spring action. The components are welded to the cell cover flange that have several electric connectors. The connectors introduce thermocouple, electric power lines for the heater and electric field supply for the sample.

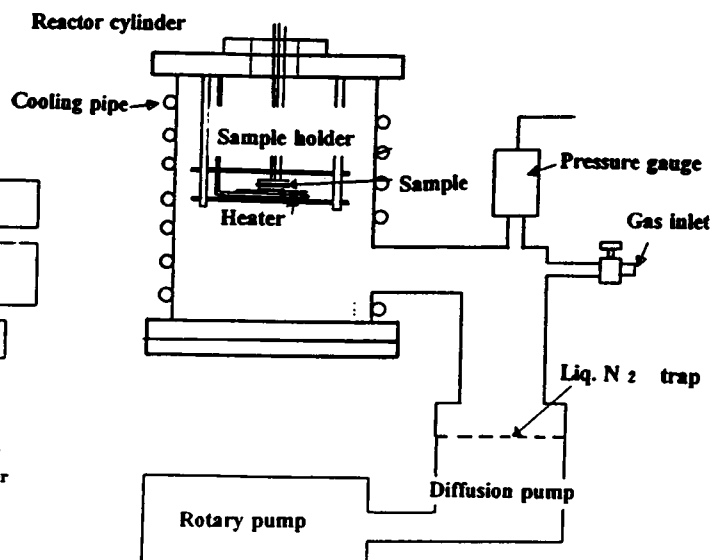
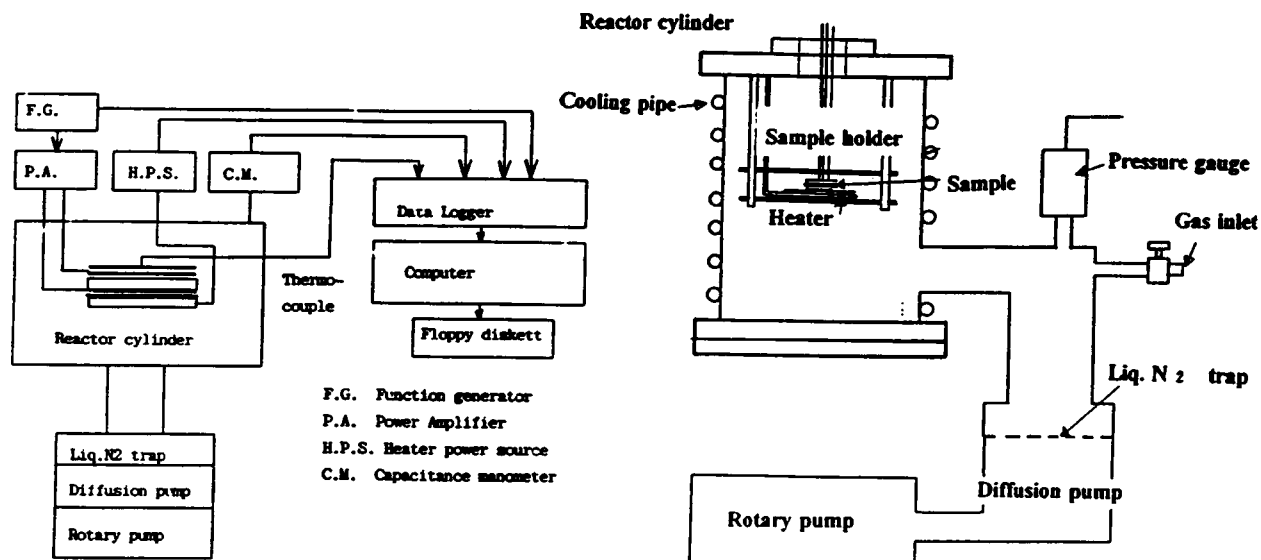


Fig. 1 Schematic representation of the measurement system.

Fig. 2 Experimental set up.

Experimental procedures are described as follows: (1) The reactor cylinder is evacuated by a rotary and diffusion pump (with liq.  $\text{N}_2$  trap) to  $2 \times 10^{-5}$  Torr. (2) Sample temperature is raised to  $400\text{-}700^\circ\text{C}$ . (3) Gas is introduced into the cylinder at 0.1-50 Torr. (4) The sample is charged with EPD power at 5-45 Volts alternating power, with frequency set between  $10^{-4}$  and 1 Hz depending on the sample temperature and thickness. (5) All the samples were analyzed for element detection by EPMA, ICP and EDS analyzer.

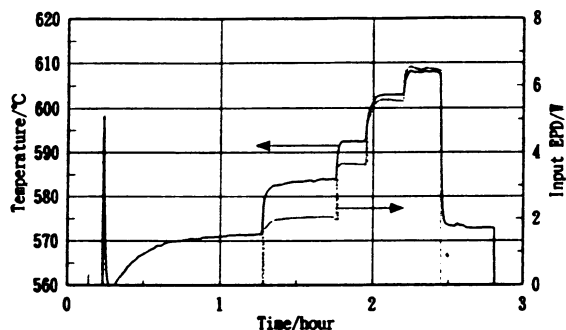


Fig. 3 Temperature change due to input EPD in  $H_2$  gas.

of  $D_2$  gas at  $500^\circ C$  with 2 cm diameter and 1 mm thickness of sample. The excess heat generation can be readily estimated from the relationship.

Fig. 3 is a typical result obtained in 13 Torr of  $H_2$  gas; this has not shown any excess heat generation. All the temperature changes are caused with input EPD deviation. However, Fig. 4 shows a relation between temperature and EPD input (a) and estimating of typical excess heat evolved (b), in 12 Torr of  $D_2$  gas. With only heater power supplied, the sample temperature rose to  $50^\circ C$  and almost stabilized. After 3 hour EPD input of  $\pm 26 V$ , 0.001 Hz was supplied. At 4.6 hours the sample temperature rose  $625^\circ C$  and excess heat was clearly generated after the time (Fig. 4b). Input EPD varied unstably and cannot be kept constant input power because the EPD currents are effected with temperature change. After the EPD power off, characteristic phenomena were seen; excess heats were evolved during an hour. Total excess heat evolution is estimated as 11 K joule.

## ANALYSIS OF ELEMENTS

All the samples, including no excess heat, were analyzed by EPMA, ICP, EDS and SEM observation. Fig. 5, for example, shows the sample surface observation by SEM; many holes and swelled parts can be seen. The EDS analysis shows the existence of Al, Sm and Gd elements around the parts. These elements exist locally near the changed parts of the sample. Fig. 6 shows the element mapping for the sample surface (a) and cross section (b) by EPMA.

## RESULTS HEAT MEASUREMENTS

The relationships between input EPD and temperature were calibrated with a dummy sample and a ceramic heater. Next relationship is obtained between temperature (T) and EPD (E) in the range from  $400$  to  $700^\circ C$  as follows:

$$E = A \exp BT \quad (1)$$

A and B are constants that are caused from gas kinds, pressure and sample dimensions. We obtained, for example,  $6.4^\circ C$  temperature rise for one watt input EPD in 10 Torr

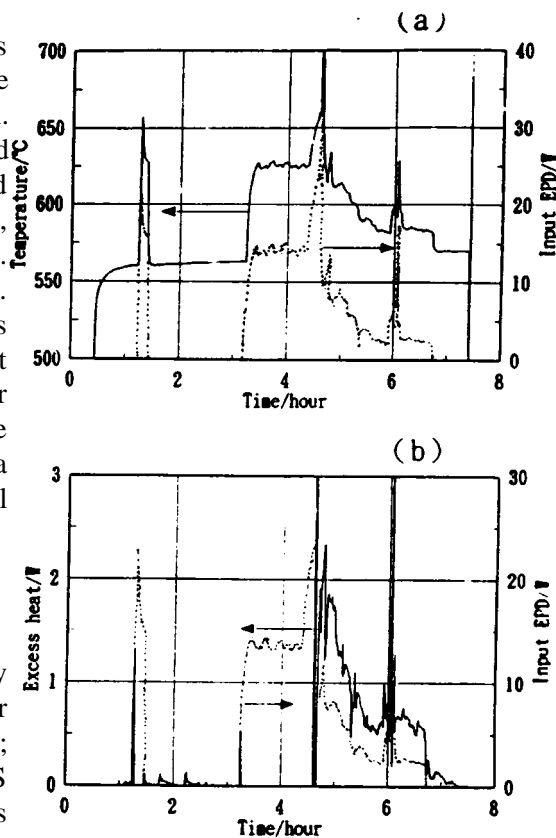


Fig. 4 Changes of temperature and EPD input in  $D_2$  gas (a), changes of excess heat (b).

Characteristic phenomenon can be seen for Sr and Ce concentrations; these concentration profiles show an opposite relation. High Sr concentration areas coincidences with low Ce concentration profile. They are a reverse profiles. Other additive elements, Nb and Y show no change and kept the same concentrations as before while Pt film is almost peeled off around the swelled and melted parts.

Aluminum exists around the changed parts at the sample and it also can be detected in the bulk layer. However, Ca is only found under the surface layer in the changed parts; it strongly segregates locally. Mg distributes widely around the changed parts and shows lower concentration than the Ca. Other lanthanides cannot be detected by the EPMA method because of their low concentration value.

Several samples were analyzed for element change by ICP method. Table 1 is the ICP result; Each case shows the average value of five for the before and the no excess heat samples and 10 of excess heat evolved samples. Significant increase can be seen for Mg, Ca, Al, Sr, Fe, Bi, Sm, Gd and Dy. Other impurities are also increased in each case; this phenomenon can be considered due to contamination from the surround. Ceramic samples are sintering material having many holes and porous; they are easily contaminated. However, former elements show clear increase after excess heat generation.

## CONCLUSION

All previous attempts at Cold Fusion experiments can be classified as either wet or dry loading of hydrogen isotopes. Contrary to previous works, the initial attempts have been done by Granite et al. (4). They thought it would be useful to combine the wet and dry methods to apply electrochemical potential in the gas phase. They employed  $\beta$ -alumina specimens for the study and sometimes observed few emission of neutrons as low as the background. The  $\beta$ -alumina is unstable at high temperature up to 300° C and shows no proton conductivity. Meanwhile, lattice type proton conductors such as perovskite oxide kept steady proton conductivity high as the temperature region around 1000° C. Excess heat usually evolved certain time lag after applying the input power. Proton mobility at the temperature is easily obtained using the Nernst-Einstein relation as follows:

$$D/RT = \sigma/nZ^2e^2 \quad (2)$$

Here,  $Z$  is charge number as 1 for  $D^+$ ,  $n$  ion density in the sample that obtained from current density. Proton mobility  $4 \times 10^{-6}$  at 450° C and  $1.05 \times 10^{-5}$  at 540° C  $cm^2/s \cdot V$  obtained by the relation are same as Yajima data (5). However, the time lag between the occurring excess heat evolution and the supply of input power is almost ten times larger than the time that obtained the relationship for the case of proton reach a side to another one. And the excess heats clearly decreased after ceased the input power supply. This phenomenon suggests that the excess heat evolution may be induced by deuterium flow in the conductor accelerated by an electric field. Only five samples in fifty showed the excess heat evolution. Also, the construction and composition of the proton conductor can be considered an important factor that decides the reaction of excess heat evolution. Clear increase of several element such as Al, Ca, Mg, Bi, Sm, Gd and Dy. It is still under consideration that the elements are reaction products of requisite existence for the Cold Fusion.

## REFERENCES

1. H. Iwahara, T. Esaka, H. Uchida and N. Meda, *Solid State Ionics*, 3/4, 359 (1981).
2. H. Iwahara, H. Uchida, K. Kondo and K. Ogaki, *J. Electrochem. Soc.*, 135, 529 (1988).
3. T. Yajima, K. Koide, K. Yamamoto and H. Iwahara, *Denki Kagaku*, 58, 547 (1990).

4. E. Granite and J. Jorne, *J. Electroanal. Chem.*, 317, 285 (1991).
5. T. Yajima, Doctoral thesis (1992).

**Table 1** ICP analysis for impurities in the samples.

Element	Before experiment	No excess heat	Excess heat evolved
Li	5 ± 0.7	5 ± 0.7	5 ± 1
Na	10 ± 1	10 ± 1	12 ± 1
Mg	5 ± 0.8	5 ± 1.2	10 ± 3
K	10 ± 0.9	10 ± 1.5	15 ± 1.8
Ca	20 ± 2	20 ± 0.8	40 ± 5
Ba	40 ± 5	40 ± 8	40 ± 10
Al	3 ± 0.2	5 ± 1	15 ± 5
Si	1.5 ± 0.1	3 ± 1	5 ± 1
Fe	0.5 ± 0.1	3 ± 1	5 ± 1
Ni	2 ± 0.1	3 ± 1	5 ± 1
Cu	0.3 ± 0.1	1 ± 1	1 ± 1
Cr	1 ± 0.1	2 ± 1	2 ± 1
Cd	0.5 ± 0.1	1 ± 0.5	1 ± 0.5
Pd	6.5 ± 1	6 ± 1	8 ± 2
Bi	0	0.1	5 ± 1
Zn	0.5 ± 0.1	1 ± 0.1	2 ± 0.2
Nd	2.5 ± 0.1	2.5 ± 0.1	4 ± 1
Sm	2.0 ± 0.1	2.0 ± 0.1	10 ± 1
Gd	0	0	5 ± 1
Dy	0	0	5 ± 1

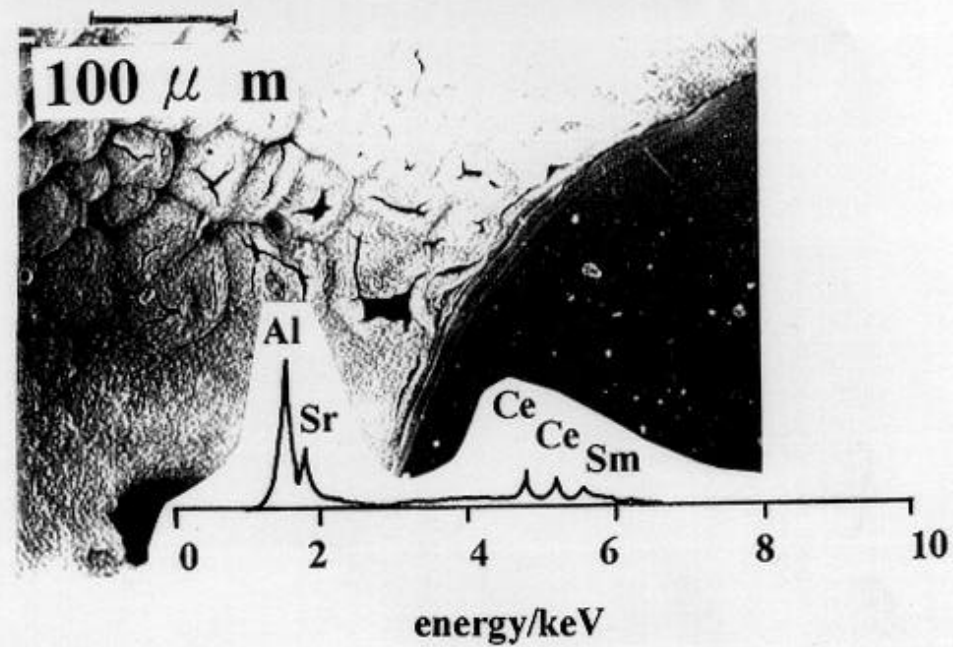
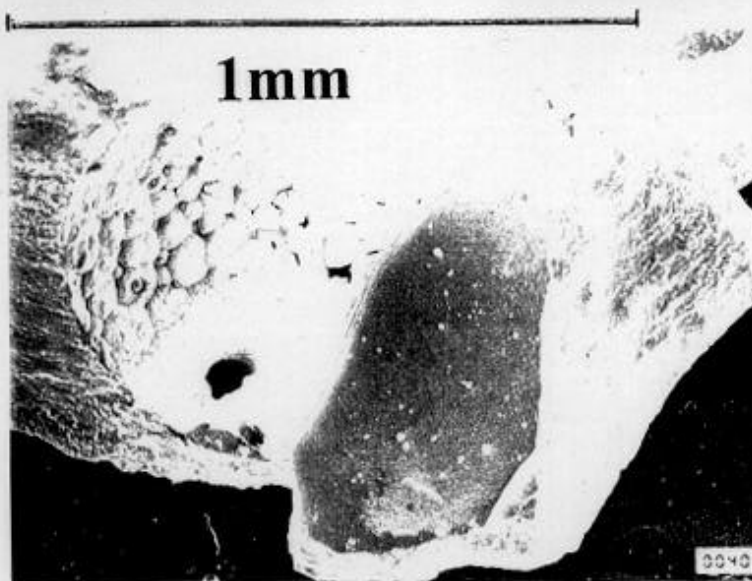
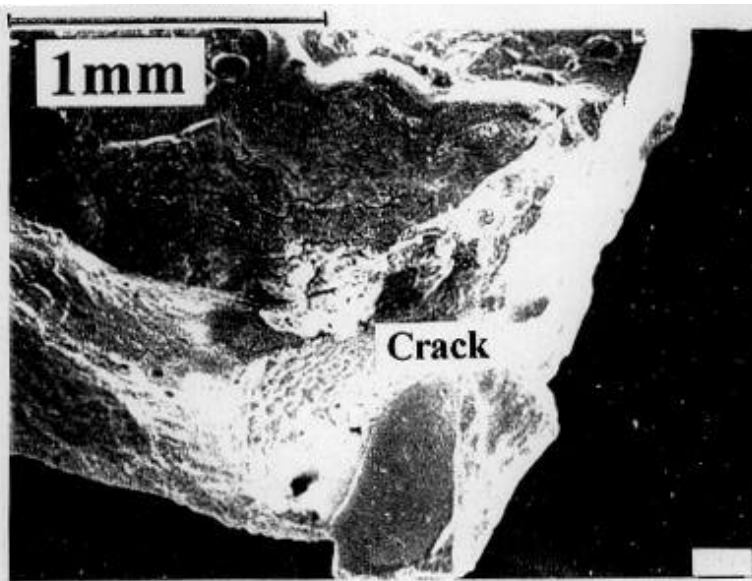
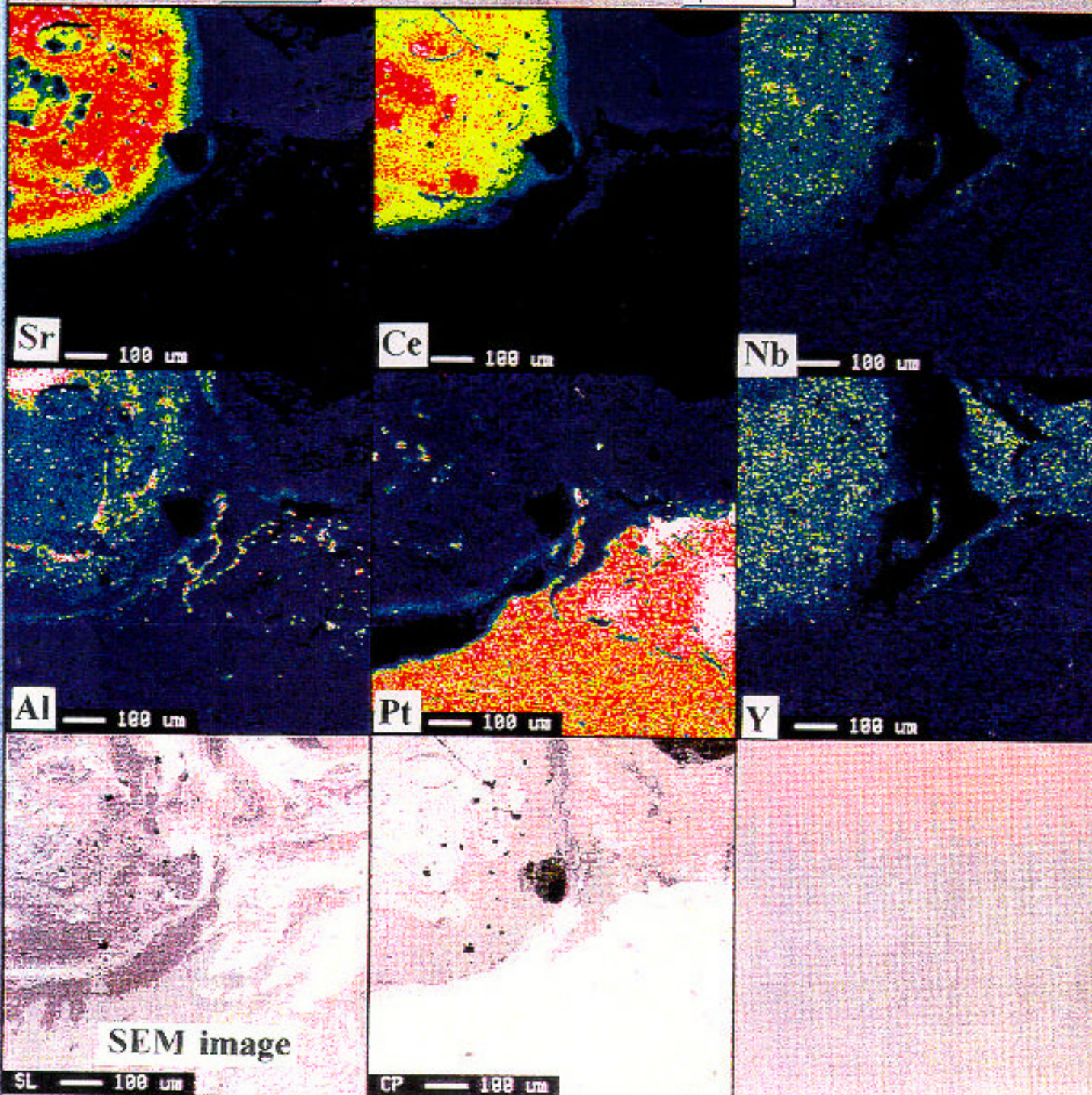


Fig.5 SEM and EDS spectroscopy observation for surface of excess heat evolved sample



Sample

Operation



Sr	Level	Ce	Level	Nb	Level
400		580		25	
371		539		23	
314		456		20	
257		373		16	
200		290		13	
143		207		9	
86		124		5	
29		41		2	
0		0		0	
Ave	85	Ave	103	Ave	3

Al	Level	Pt	Level	Y	Level
50		50		20	
46		46		19	
39		39		16	
32		32		13	
25		25		10	
18		18		7	
11		11		4	
4		4		1	
0		0		0	
Ave	8	Ave	18	Ave	3

SL	Level	CP	Level
1595		1256	
1526		1663	
1387		1477	
1248		1290	
1110		1104	
971		918	
832		731	
693		545	
624		452	
Ave	1073	Ave	1135